

Remarks on the Proton Structure

E. Comay*

Charactell Ltd.

PO Box 39019

Tel-Aviv, 61390 Israel

PACS No: 03.30.+p, 03.50.De, 12.90.+b, 13.85.Dz

Abstract:

Elastic and inelastic cross section of proton-proton and electron-proton scattering are discussed. Special attention is given to elastic scattering and to the striking difference between the data of these two kinds of experiments. It is shown that the regular charge-monopole theory explains the main features of the data. Predictions of results of CERN's Large Hadron Collider are pointed out.

1. Introduction

Scattering experiments are used as a primary tool for investigating the structure of physical objects. These experiments can be divided into several classes, depending on the kind of the colliding particles. The energy involved in scattering experiments has increased dramatically during the century elapsed since the celebrated Rutherford experiment has been carried out. Now, the meaningful value of scattering energy is the quantity measured in the rest frame of the projectile-target center of mass. Therefore, devices that use colliding beams enable measurements of very high energy processes. For this reason, the Large Hadron Collider (LHC) facility at CERN, which is designed to produce 14 TeV proton-proton (pp) collisions, will make a great leap forwards.

This work examines two different scattering data of protons. One set consists of the pre-LHC pp scattering data and the second set is electron-proton and positron-proton scattering data. Hereafter, ep denote these lepton-proton scattering experiments. A special attention is given to elastic scattering (ES), where the proton remains intact and no new particle is produced. The data prove that the elastic cross section (ECS) of pp scattering differs dramatically from that of ep . These experimental data are explained by the Regular Charge-Monopole Theory (RCMT). It is also shown how this theory together with currently available data yields a prediction of LHC results.

The Lorentz metric used is diagonal and its entries are (1,-1,-1,-1). Expressions are written in units where $\hbar = c = 1$. In this system of units there is just one dimension. Here it is taken to be that of length. Therefore, the dimension of a physical quantity is a power of length and is denoted by $[L^n]$.

The data on cross sections of pp and ep are presented in the second Section. An analysis of these data and a theoretical explanation of their main features are included in the third Section. The fourth Section discusses the structure of the baryonic core.

The last Section contains concluding remarks.

2. The Relevant Cross Section Data

Let us turn to the pp scattering (see fig. 1 and its original version [1]). Points A , B , C divide the ECS graph into four parts. For a laboratory momentum smaller than that of point A , the elastic cross section shows the characteristic decreasing pattern of a Mott-like scattering.

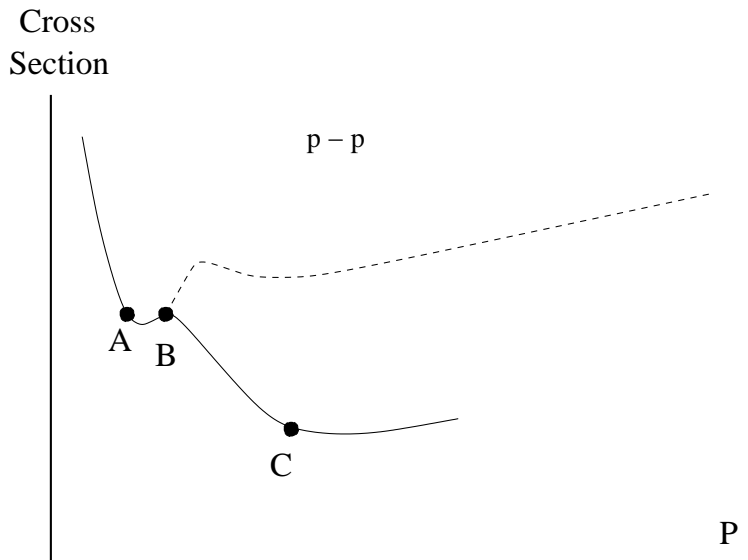


Figure 1: *Proton-proton cross section versus the laboratory momentum P . Axes are drawn in a logarithmic scale. The continuous line denotes elastic cross section and the broken line denotes total cross section. Points A, B, C help the discussion (see text). (The accurate figure can be found in [1]).*

Clearly, the Mott-like decrease of the cross section does not hold for a momentum greater than that of point A . For the momentum interval $[A, B]$, a new force enters the scattering process. This is the nuclear force whose phenomenological properties are well known for a very long time [2]. Its main features are a quite strong repulsive force at the nucleon's inner part and an attractive force outside it. The nuclear

attractive force decays more rapidly than the Coulomb force. At a short distance from the proton's center, these forces are much stronger than the electromagnetic force. (The fact that near the origin the potential of the nuclear force $V(r)$ varies more rapidly than the potential of the Coulomb force $1/r$, is significant. This point is discussed in the third Section.) For momentum values belonging to the interval $[A, B]$, the nuclear force alters the direction of the graph that describes ECS. Here the decrease of ECS stops continuously and for a certain interval of the projectile's momentum, ECS increases with it.

Let us examine the momentum interval belonging to points $[B, C]$. Fig. 1 indicates that a new process begins to take place for momentum values greater than that of point B . For these values, the collision's energy is large enough for producing hadrons. It means that inelastic scattering begins at point B . The inelastic cross section (ICS) is the difference between the broken line describing the total cross section (TCS) and the continuous line describing ECS. Thus, for momentum values greater than that of point B , ECS begins to decrease. An examination of the scale of the original figure [1] indicates that ICS becomes greater than ECS and at point C , ICS is about five times greater than ECS.

For momentum values greater than that of point C , the decreasing pattern of ECS gradually stops and it slightly begins to increase together with the momentum. It can be concluded that points A, B, C of the graph show clearly four momentum regions, each of which has a unique behavior of ECS.

In the second kind of scattering data, one proton is replaced by an electron. Unfortunately, in the case of ep scattering, publications of Particle Data Group, like [1], do not contain a figure which is analogous to fig. 1. Therefore, the discussion relies on appropriate formulas that describe the data. The following arguments prove that in ep scattering, the characteristics of the cross section differ substantially from the pp data depicted in fig. 1.

Let us examine the elastic ep scattering. In this case the analysis uses the Rosenbluth formula. Here the Mott cross section is factored out and is multiplied by trigonometric functions and form factors which depend on the square of the 4-momentum transferred q^2 . The Mott differential cross section takes the following form (see [3], p. 192)

$$\left(\frac{d\sigma}{d\Omega}\right)_{Mott} = \frac{\alpha^2 \cos^2(\theta/2)}{4p^2 \sin^4(\theta/2)[1 + (2p/M) \sin^2(\theta/2)]}, \quad (1)$$

where $\alpha \simeq 1/137$ denotes the square of the electron's charge and p is the linear momentum of the incoming electron. The Rosenbluth formula can be cast into the following form (see [3], p. 193, eq. (6.26))

$$\left(\frac{d\sigma}{d\Omega}\right)_{Rosenbluth} = \left(\frac{d\sigma}{d\Omega}\right)_{Mott}(A(q^2) + B(q^2) \tan^2(\theta/2)), \quad (2)$$

where A and B are related to the proton's electric and the magnetic form factors.

In the ep case, the Rosenbluth formula (2) is used for describing ECS. This formula is valid even for the very high energy of modern colliders [4]. A useful quantity is called the dipole form factor (see [3], p. 196)

$$G_D(q^2) = (1 + q^2/0.71)^{-2}, \quad (3)$$

where q^2 is measured in GeV^2 . It turns out that, for all energies used up to date, the actual form factors are nearly the same as (3). For the present discussion it is sufficient to realize that the actual form factors are of the same order of magnitude as (3) (see figures 2,3 of [5]). It can be concluded that the ep elastic form factor decreases with an increase of q^2 and for $q^2 \gg 1 \text{ GeV}^2$, the contribution of the electric form factor G_E decreases like q^{-4} and that of the magnetic form factor decreases like q^{-2} (see [3], p. 193). Moreover, these decreasing contributions are multiplied by the Mott cross section that decrease like p^{-2} .

The form of the deep inelastic cross section is quite different. Using the notation

of [3], sections 8.2 and 8.3, one finds for deep inelastic collisions

$$\left(\frac{d^2\sigma}{dq^2 dx}\right) = \frac{4\pi\alpha^2}{q^4} \left[(1-y) \frac{F_2(x, q^2)}{x} + y^2 F_1(x, q^2) \right]. \quad (4)$$

Here x and y are dimensionless variables whose value falls in the range $[0,1]$. Experimental evidence proves that Bjorken scaling holds and that the expression inside the square brackets of (4) is very nearly independent of q^2 . Hence, integrating (4) on q^2 , one finds that the deep inelastic cross section decreases like $1/q^2$. This is the rate of the decrease of the magnetic form factor contribution to the elastic scattering.

The first interesting issue is the ratio of ECS to TCS which is found for very high energy. As stated above, in the case of pp scattering, this ratio is about $1/6$. On the other hand, the additional $1/p^2$ factor of the Mott cross section (1) proves that in ep scattering, elastic events are very rare. Hence, the data lead one to the following conclusion:

- I. For very high energy, about 16% of the pp scattering events are elastic whereas in the corresponding ep scattering, the percentage of elastic events is very, very small.

The second issue is the behavior of ECS as a function of energy in the two kinds of scattering experiments described above. The data of fig. 1 (see [1]) shows how the pp cross section varies as a function of either the projectile's momentum or, equivalently, on a different scale, as a function of \sqrt{S} , where S is the square of the invariant energy of the colliding particles.

The ECS graph of fig. 1 shows that it stops decreasing for energies which are somewhat greater than that of point C . In the case of the ep scattering, the ECS information is given in terms of the differential cross section which depends on the invariant square of the momentum transferred q^2 . However, the following calculation proves that for ep scattering ECS does not stop decreasing with the increase of the collision's energy.

The calculation is carried out in the rest frame of the colliding particles. Let the 4-momentum of the incoming electron be

$$p_{in}^\mu = (\sqrt{p^2 + m^2}, 0, 0, p) \quad (5)$$

and that of the outgoing electron is

$$p_{out}^\mu = (\sqrt{p^2 + m^2}, p \sin \theta, 0, p \cos \theta). \quad (6)$$

It follows that the square of the momentum transferred is

$$q^2 = (p_{in}^\mu - p_{out}^\mu)(p_{\mu in} - p_{\mu out}) = 2p^2(1 - \cos \theta). \quad (7)$$

Now the elastic cross section σ is the spherical integral of the Rosenbluth differential cross section formula (2)

$$\sigma = \int \left(\frac{d\sigma}{d\Omega} \right)_{Rosenbluth} \sin \theta d\theta d\phi. \quad (8)$$

Let us examine the integrand of (8) at a certain value of (θ, ϕ) . Relation (7) proves that a replacement of q^2 by p^2 is followed by a trigonometric factor. Now if p increases then the Mott factor (1) decreases and the same is true for the dipole factor (3). Therefore, since the differential cross section is positive and it decreases for all values of (θ, ϕ) , one concludes that the spherical integral (8) also decreases with increasing momentum. This outcome proves that for the ep scattering discussed here, ECS does not stop decreasing with an increase of the linear momentum. The validity of the following conclusion relies on these results.

II. For high enough energy there is a substantial difference between elastic scattering of pp and of ep . If the collision energy increases then ECS of pp stops decreasing and even shows a small increase whereas ECS of ep does not stop decreasing.

There is another kind of difference between ep and pp scattering. The Mott formula decreases like $1/p^2$. This matter is evident on the basis of dimensions arguments. The cross section has the dimension $[L^2]$. In the system of units used here, energy and momentum have the dimension $[L^{-1}]$ and the coupling constant α is dimensionless. This argument explains the negative slope of the cross section $\sigma(p^2)$ of the Mott formula (1) and of the deep inelastic scattering of ep (4).

This property does not hold for the pp scattering. Here one sees that for low momentum, which is smaller than that of point A of fig. 1, The TCS decreases steeply, as expected from the Mott formula. Let us turn to momentum values which are greater than that of point A of fig. 1, For most of these momentum regions, TCS increases and at a short region of momentum values, it decreases. However, the decrease rate is much smaller than the quite steep slope of $1/p^2$. Therefore, it is concluded that

- III. Unlike the case of ep scattering, one finds that for high enough energy, TCS of pp does not follow the $1/p^2$ decrease of the Mott formula..

Physical consequences of conclusions I-III of this Section are discussed in the rest of this work.

3. A Discussion of the Cross Sections

The pp and ep scattering experiments help us understand the proton's structure. Conclusions I-III of the previous Section reveal a dramatic difference between the results of these experiments. For example, experiments done in the HERA facility at DESY report on ep collisions where $q^2 > 10000 \text{ GeV}^2$ [6-8]. Substituting these values of q^2 in the dipole formula (3), and remembering that the magnetic form factor

dominates very high q^2 collisions, one finds that for ep scattering the ratio of ECS to ICS is less than 10^{-4} . On the other hand, in the pp scattering this ratio is about $1/5$. These properties are important for the discussion carried out below. Therefore, they are summarized as follows:

1. For nearly all events of energetic collisions of electrons with proton's quarks, the proton is broken apart and the fragments come out as a set of hadrons. The relative number of elastic collisions where the proton remains intact is very, very small.
2. In pp collision of similar energy, about 16% of the events are elastic and in these cases the proton remains intact.

The following explanation of properties 1,2 is adopted here:

- a. The proton consists of quarks and of another object called baryonic core. The existence of the baryonic core is consistent with the experimental evidence showing that for an ultra-relativistic proton, quarks carry just about one half of the proton's linear momentum (see [3], p. 282).
- b. The baryonic core is electrically neutral. Therefore, electrons do not interact with it. (Conditions for a possible deviation from this behavior are discussed in the next Section.)
- c. The baryonic core participates in strong interactions. Hence, three kinds of interacting pairs of particles exist in a very high energy pp collision: quark-quark, quark-core and core-core.
- d. The core is a relatively rigid object and a core-core interaction is likely to produce an elastic collision.

Statements a-d make a phenomenological explanation of the data discussed in this work in general and of points 1,2 in particular. Thus, in a pp collision there is a core-core interaction. The relative rigidity of the core is the primary reason for the non-negligible part of ECS in pp collision. The fact that the core is electrically neutral explains why it does not contribute to ECS of ep collisions. The following lines present a theoretical basis for points a-d..

It has been proved that one can use very well established physical principles and construct a regular theory of electric charges and magnetic monopoles RCMT [9,10]. The main results of RCMT can be put in the following words:

Charges do not interact with bound fields of monopoles and monopoles do not interact with bound fields of charges. Charges interact with all fields of charges and with radiation fields emitted from monopoles. Monopoles interact with all fields of monopoles and with radiation fields emitted from charges. Another important result of RCMT is that the unit of the elementary magnetic charge g is a free parameter. However, hadronic data indicate that this unit is much larger than that of the electric charge $g^2 \gg e^2 \simeq 1/137$. More details of RCMT can be found in [9-11].

These properties of RCMT fit like a glove the data of electromagnetic projectiles interacting with nucleons (see [11], pp. 90-92). Thus, protons and neutrons do not look alike in cases of charged lepton scattering whereas they look very similar if the projectile is a hard enough real photon (see [12] and the figure on p. 369 of [1]).

Electrodynamics of magnetic monopoles is dual to electrodynamics of electric charges. This analogy is helpful for understanding the applicability of RCMT to hadrons in general and to baryons in particular. Baryons do not show the static force that should be found between monopoles. Therefore, one must assume that they are neutral with respect to magnetic charge. Thus, each quark is assumed to carry one negative unit of monopole. The overall monopole charge of baryons vanishes because the baryonic core carries three positive units of magnetic charge. (The relative sign

of the monopole charge of quarks and of the baryonic core is arbitrary. Here it is defined so that the similarity with the respective electric charge of electrons and nuclei holds.) The elementary unit of magnetic charge is much larger than that of the electric charge. For this reason, baryonic quarks are very tightly bound to the core (provided the comparison is made with atomic electrons). Therefore, a baryon can be regarded as a magnetic monopole analog of an atom, where quarks are strongly bound to the core. A quark is analogous to an electron and the baryonic core is analogous to the atomic nucleus.

Now let us use this structure of baryons together with very well established physical principles for an interpretation of a pp scattering process. The discussion is carried out in the rest frame of one proton (the target). The projectile interacts with the static potential of the target. As the linear momentum of the projectile increases, its wave length decreases and its wave function changes sign more rapidly. Therefore, spatial regions where the potential varies slowly make a very small contribution to the scattering of very high energy. This general quantum mechanical argument proves that for a very short wave length of the projectile, a meaningful contribution to the scattering process is obtained only from the region near the baryonic core, where the potential varies strongly.

Another point which is relevant to the discussion is the $1/r$ variation of the Coulomb potential. This kind of variation leads to the Rutherford and the Mott (1) scattering formulas, where the cross section falls like p^{-2} . Therefore, a TCS rise of more energetic pp scattering must be related to a potential whose spatial variation is stronger than the Coulomb $1/r$ value. This requirement holds for the two regions of fig. 1 where the cross section increases: the regions where the momentum is larger than that of points A, C , respectively.

Let us begin with momentum values which are smaller than that of point B of fig. 1. For momentum values which are smaller than that of point A of fig. 1, one

finds a typical Mott-like $1/p^2$ decrease of the cross section. Let us turn to momentum values of the interval $[A, B]$. Here the nuclear force enters the process. Relative to the Coulomb force, this force varies very rapidly at the spatial region where it is not negligible. Therefore, the increase of TCS between points $[A, B]$ is understood. For momentum values greater than that of point C , a similar effect is found inside the proton. Indeed, one should remember that by analogy with atomic structure, valence quarks screen the core's potential. Therefore, as a particle (either a quark or the core of the projectile) approaches the baryonic core of the target, the interaction increases more rapidly than the $1/r$ rate of a Coulomb potential. Hence, the contribution of the quark-core and core-core interaction increases. The former mainly affects ICS and the latter mainly affects ECS. Thus, for an energy greater than that of point C of fig. 1, the increase of both TCS and ECS is also understood.

4. The Structure of the Baryonic Core

Up to this point, the discussion relies only the fact that the baryonic core carries three units of monopole charge. (This property is mandatory for RCMT, because of the need to explain the neutrality of baryons with respect to magnetic charge.) Referring to the problem of the core's structure, one may consider two alternatives:

1. The core is a simple elementary pointlike object.
2. The core contains closed shells of quarks.

The first case is certainly simpler than the second case. However, one should not expect to find that Nature is too simple. In particular, there are two different experimental data that support the second case.

The experiments carried out in the HERA facility at DESY [6-8] report that the

number of events of very high q^2 ep scattering is more than expected. This result can be explained as an analog of the Franck-Hertz experiment: interaction with bound particles takes place only if the projectile's energy is high enough. In the present discussion, the bound particles are quarks of closed shells of the baryonic core. A different kind of data is the charge radius of the proton and that of the π^\pm meson. It can be shown why these data provide two different arguments supporting the existence of closed shells of quarks at the baryonic core [13]. On the basis of these experiments, it is assumed here that the baryonic core has closed shells of quarks. Let us see how this assumption is expected to affect results of CERN's LHC.

The HERA experiments also provide information on the energy required for exciting quarks belonging to the baryonic core. This statement relies on [6-8] whose results are explained by this kind of excitation. At HERA, the proton, energy is 820 GeV and that of the positron is 27.5 GeV [7]. Obviously, for these ultra-relativistic values, these numbers also represent the linear momentum. At LHC, a proton replaces HERA's positron. Here a rough comparison of the collision energy of these colliders is described. The evaluation uses an appropriate replacement of the positron, which is an elementary pointlike particle, by one of the protons that participate in the LHC collision. Thus, let P denote an LHC proton that corresponds to a proton at HERA and P' denotes an LHC proton that replaces HERA's positron. Now, we know that in an ultra-relativistic proton, valence quarks together with the additional $\bar{q}q$ pairs carry about one half of the proton's momentum (see [3], p. 282). Hence, all quarks of P' carry kinetic energy of 3500 GeV and each quark of P' carries about 800 GeV of kinetic energy. (This estimate relies on the fact that beside the three valence quarks, there is a nonvanishing probability that the proton contains $\bar{q}q$ pairs.) These arguments show that at LHC, the energy of the proton P is more than eight times larger than that of HERA's proton and the energy of each quark of LHC's P' is about 30 times larger than that of HERA's positron. It follows that at LHC, collisions with

the baryonic core will be much more energetic than those of HERA.

Relying on this analysis, one can predict that the number of energetic LHC events will be more than those which are expected on the basis of the present knowledge of valence quarks and of the $\bar{q}q$ pair. Obviously, excited quarks of the core are expected to behave like valence quarks and contribute mainly to an inelastic process. In other words, for this gigantic energy, the baryonic core stops behaving as a rigid object. These arguments lead to the following predictions of LHC results:

1. For very energetic LHC collisions, more inelastic events will be found (comparing to the collider's data of [1]).
2. This increase of the number of inelastic events will be accompanied by a *decrease* of the number of elastic events.

5. Conclusions

This work discusses the striking difference between high energy ep scattering and pp scattering data. Elastic events are very, very rare in high energy ep scattering. Therefore it is concluded that if a valence quark (or a member of a $\bar{q}q$ pair) is hit by an energetic projectile then an inelastic event follows.

In the corresponding pp scattering, elastic events are about 1/5 of the number of inelastic events. Hence, the relative portion of elastic events is larger by several orders of magnitude than that of the corresponding events of ep scattering. Therefore, one must look for another component included in the proton. This component must be rigid enough for absorbing the energy exchanged in a high energy collision without causing a proton disintegration into a set of hadrons. Since this component is not

detected by electrons (and not by positrons), it must be electrically neutral. This proton component is called here the baryonic core.

The existence of a baryonic core is a self-evident result of the Regular Charge-Monopole Theory. Therefore, the experimental data discussed in this work provide another support for the applicability of this theory to hadrons. (See [11] for other arguments of this kind.)

It is also explained why one should expect that the baryonic core contains closed shells of quarks. The HERA data indicate that the LHC energy is higher than the energy required for exciting quarks of the baryonic core. Therefore, the first prediction made at the end of the previous Section says that the very energetic collisions of the LHC will produce more inelastic events than expected on the basis of present collider data of valence quarks. A support for this prediction can be found in the highest part of [1], which is based on cosmic ray experiments. A second prediction says that the increase of the number of inelastic events will be followed by a decrease of the number of elastic events. An LHC confirmation of these predictions will provide another support for the relevance of the Regular Charge-Monopole Theory to strong interactions.

References:

* Email: elicomay@post.tau.ac.il

Internet site: <http://www.tau.ac.il/~elicomay>

- [1] C. Amsler et al., Phys. Lett. **B667**, 1 (2008). (See p. 364).
- [2] A. deShalit and H. Feshbach, *Theoretical Nuclear Physics* (John Wiley, New York, 1974). Vol 1, pp. 11-18.
- [3] D. H. Perkins, *Introduction to High Energy Physics* (Addison-Wesley, Menlo Park CA, 1987).
- [4] I. A. Qattan et al., Phys. Rev. Lett., **94**, 142301 (2005).
- [5] H. Gao, Int. J. Mod. Phys. E **12**, 1 (2003).
- [6] C. Adloff et al. *Z. Phys. C* **74**, 191 (1997).
- [7] J. Breitweg et al. *Z. Phys. C* **74**, 207 (1997).
- [8] A. Wagner *Tr. J. of Physics* **22** 525 (1998).
- [9] E. Comay *Nuovo Cimento B* **80**, 159 (1984).
- [10] E. Comay *Nuovo Cimento B* **110**, 1347 (1995).
- [11] E. Comay *A Regular Theory of Magnetic Monopoles and Its Implications in Has the Last Word Been Said on Classical Electrodynamics?* ed. A. Chubykalo, V. Onoochin, A. Espinoza and R. Smirnov-Rueda (Rinton Press, Paramus, NJ, 2004).
- [12] T. H. Bauer, R. D. Spital, D. R. Yennie and F. M. Pipkin *Rev. Mod. Phys.* **50**, 261 (1978).
- [13] E. Comay (unpublished). See: <http://www.tau.ac.il/elicomay/LHC.pdf>